Electron spin resonance studies on the organic linear-chain compounds $(TMTCF)_2X$ (C=S,Se; X=PF_6,AsF_6,ClO_4,Br)

M. Dumm and A. Loidl
Experimentalphysik V, Universität Augsburg, Universitätsstrasse 1, D-86135 Augsburg, Germany

B. W. Fravel, K. P. Starkey, and L. K. Montgomery
Department of Chemistry, Indiana University, Bloomington, Indiana 47405

M. Dressel
Experimentalphysik V, Universität Augsburg, Universitätsstrasse 1, D-86135 Augsburg, Germany
and 1. Physikalisches Institut, Universität Stuttgart, Pfaffenwaldring 57, D-70550 Stuttgart, Germany
(Received 22 April 1999)

We have conducted comprehensive electron spin resonance (ESR) investigations on single crystals of the one-dimensional organic compounds $(TMTTF)_2PF_6$, $(TMTTF)_2ClO_4$, $(TMTTF)_2Br$, $(TMTSF)_2PF_6$, and $(TMTSF)_2AsF_6$ in the temperature range from 4 to 500 K and additionally, $(TMTSF)_2ReO_4$ and $(TMTSF)_2ClO_4$ at room temperature. In contrast to the selenium analogs TMTSF which are one-dimensional metals, the sulfur salts are semiconductors with localized spins on the TMTTF dimers. Taking into account the thermal expansion of the crystals at high temperature ($T>20$ K) the ESR intensity of all sulfur compounds can be described as a spin-1/2 antiferromagnetic Heisenberg chain with exchange constants $420 \leqslant J \leqslant 500$ K. Although the TMTSF compounds are one-dimensional organic metals down to 10 K, the temperature dependence of the spin susceptibility can also be described within the framework of the Hubbard model in the limit of strong Coulomb repulsion with $J \approx 1400$ K. By modeling $(TMTTF)_2ClO_4$ as an alternating spin chain, the change of the alternation parameter at the first-order phase transition ($T_{AO}=72.5$ K) indicates a tetramerization of the chain. $(TMTTF)_2PF_6$ undergoes a spin-Peierls transition at $T_{SP}=19$ K which can be well described by Bulaevskii's model with a singlet-triplet gap $\Delta_\sigma(0)=32.3$ K. We find evidence of antiferromagnetic fluctuations at temperatures well above the magnetic ordering in $(TMTTF)_2Br$, $(TMTSF)_2PF_6$, and $(TMTSF)_2AsF_6$ which follow the critical behavior expected for three-dimensional ordering. $(TMTTF)_2PF_6$ and $(TMTTF)_2Br$ show one-dimensional lattice fluctuations.

I. INTRODUCTION

With the recent discovery of the *inorganic* spin-Peierls systems $CuGeO_3$ (Ref. 1) and α'-NaV_2O_5,[2] one-dimensional spin systems draw much attention. In this new context, it seems worthwhile to revisit the low-dimensional *organic* spin chains since these compounds provide the opportunity to nicely tune the system from itinerant to localized electrons and spins. Different ground states — like charge-density wave (CDW), spin-Peierls (SP), spin-density wave (SDW), or superconductivity — can be reached depending on the external pressure or magnetic field. In this paper we concentrate on the spin dynamics of single crystals of $(TMTTF)_2X$ and compare them with the Bechgaard salts $(TMTSF)_2X$, where TMTSF is tetramethyltetraselenafulvalene, TMTTF denotes tetramethyltetrathiafulvalene, and $X=PF_6$, AsF_6, ClO_4, ReO_4, or Br stands for a monovalent anion. As seen in the phase diagram Fig. 1, by changing the anions X, or slightly modifying the organic molecule TMTCF, where C is one of the chalcogenes S, Se, or Te, the chemical pressure and therefore the magnetic and electronic properties can easily be modified.[3,4]

First let us briefly summarize some of the physical properties of these organic linear chain compounds. Based on electron counting arguments, the TMTCF salts are metals with a formally 3/4 filled conduction band. The actual band filling, however, is 1/2 due to a weak dimerization along the chains; further modifications may be caused by electronic correlations. While $(TMTSF)_2ClO_4$ is the only compound which at ambient pressure stays metallic down to 1 K where it becomes superconducting, most of the other Bechgaard salts undergo a metal-to-insulator transition (at temperatures around 10 K) which in some cases like $(TMTSF)_2PF_6$ can be suppressed by external pressure (Fig. 1). Due to the larger anisotropy, stronger dimerization, and larger on-site Coulomb repulsion the TMTTF salts are closer to the Mott-Hubbard insulating state. $(TMTTF)_2PF_6$ is known to be the most correlated compound of the sulfur series. In the phase diagram $(TMTTF)_2Br$ lies between $(TMTSF)_2PF_6$ and $(TMTTF)_2PF_6$ since superconductivity has been observed only under very high pressure. Much less is known about $(TMTTF)_2ClO_4$, but it takes a position somewhere between $(TMTTF)_2PF_6$ and $(TMTTF)_2Br$.

Structural considerations are of superior importance for the understanding of the differences between the various TMTCF salts; for a recent review see Ref. 5. The organic molecules are stacked along zigzag chains in the a direction separated in the c direction by the anions. The slight dimerization of the molecules can best be expressed by the intrastack intermolecular transfer integrals as listed in Table I.

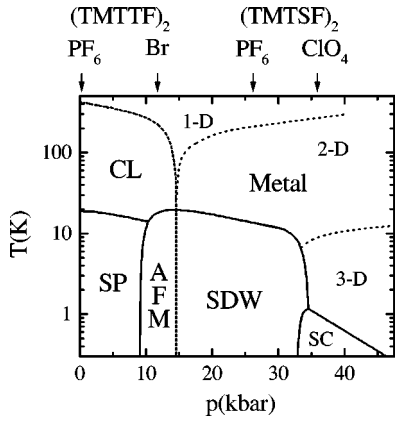

FIG. 1. Phase diagram of the TMTSF and TMTTF salts after Refs. 3 and 4 determined for example by pressure-dependent resistivity measurements. For the different compounds the ambient-pressure position in the phase diagram is indicated. Going from the left to the right, the material gets less one-dimensional due to the increasing interaction in the second and third direction. CL stands for charge localization, SP for spin-Peierls, AFM for antiferromagnet, SDW for spin-density wave, and SC for superconductor.

The dimerization decreases as PF_6 is replaced by ClO_4 and going from the selenium compounds to the sulfur counterparts.

Unlike the selenium analogs which in general are metallic down to low temperatures, the TMTTF salts discussed here are Mott-Hubbard insulators due to the small transfer integrals (Table I). Consequently they show a broad but distinct resistivity minimum at high temperatures[9,10] attributed to the opening of a charge gap Δ_ρ.[11] Since x-ray studies show no indications of a $4k_F$ charge-density wave,[5] it is considered to be a continuous $4k_F$ charge localization due to the anion potential (lattice dimerization). Thus the amplitude of the charge gap is closely connected to the dimerization and $\Delta_\rho \approx 600$ K for $(TMTTF)_2PF_6$. The charge gap is estimated[12] to be $t_a/2$ in $(TMTTF)_2PF_6$ but only $t_a/25$ in $(TMTSF)_2PF_6$, where $t_a=(t_{a_1}+t_{a_2})/2$ is the average transfer integral along the stacks. This gap enhancement is due to the increased Coulomb interaction and the increased dimerization. By applying pressure on $(TMTTF)_2PF_6$ the resistivity minimum decreases in temperature and at 13 kbars the salt is fully metallic and undergoes a SDW phase transition similar to $(TMTSF)_2PF_6$.[13,6,14] Applying pressure also enhances the interchain coupling, in agreement with the fact that $(TMTTF)_2PF_6$ is more one dimensional than the selenium analog (Fig. 1).

$(TMTTF)_2Br$ is close to the borderline between itinerant and localized carriers: only below 100 K the resistivity increases due to charge localization. As a consequence, the transition to an antiferromagnetic ground state at 13 K does not lead to a SDW, as observed in $(TMTSF)_2PF_6$ which stays metallic down to T_{SDW}, but to a localized antiferromagnet (AFM).

It is known from transport,[10] susceptibility,[15] NMR,[13] and x-ray[16] measurements that $(TMTTF)_2PF_6$ undergoes a SP transition at $T_{SP} \approx 19$ K. Below approximately 50 K the opening of a pseudogap is inferred from the reduction of the spin susceptibility and ^1H and ^{13}C NMR relaxation rate.[13,17] X-ray data also show a $2k_F$ superstructure below 60 K.[16,5]

TABLE I. Parameters of the intermolecular intrastack transfer integrals $\Delta t_a/t_a=2(t_{a_1}-t_{a_2})/(t_{a_1}+t_{a_2})$, the interstack transfer integral t_b, and $\gamma_C=|C-C|_{vdW}/|C-C|_{min}$ (after Refs. 6–8) compared with ESR results on the linewidth and the g shift, whereas $\overline{\Delta H}=(\Delta H_a+\Delta H_{b'}+\Delta H_{c*})/3$ and $\overline{\Delta g^2}=(\Delta g_a^2+\Delta g_{b'}^2+\Delta g_{c*}^2)/3$. All data are given at room temperature.

		$(TMTTF)_2X$			$(TMTSF)_2X$			
X		PF_6	ClO_4	Br	PF_6	ReO_4	AsF_6	ClO_4
t_{a_1} (meV)		137	140	133	252	248		258
t_{a_2} (meV)		93	100	119	209	215		221
$\Delta t_a/t_a$		0.38	0.33	0.11	0.19	0.14		0.15
t_b (meV)		12.3		12.4	33.5			27.0
γ_C		0.93	0.93	0.99	1.03	1.04	1.03	1.06
ΔH (Oe)	a	2.53	2.82	4.26	161.9	160	179	206.3
	b'	3.11	3.41	5.31	205.5	215	197	250.6
	$c*$	3.86	4.27	6.03	229.4	244	214	289.4
Δg (10^{-3})	a	-0.9	-1.3	-0.9	-11.0	-10	-10	-10.5
	b'	5.9	5.8	6.0	27.1	28	27	28.5
	$c*$	8.0	7.9	7.7	39.5	40	39	40.7
$\overline{\Delta H}/\overline{\Delta g^2}$ (kOe)		95.5	107.4	162.5	247.0	249	251	289.4

These findings are in contrast to earlier results by Coulon *et al.*[10] who only found the susceptibility vanishing below 15 K.[18] The g factor is temperature independent in all three directions. The linewidth decreases with T in the high-temperature phase of $(TMTTF)_2PF_6$.

The phase transition of $(TMTTF)_2ClO_4$ at $T_{AO}=72.5$ K is driven by the ordering of the noncentrosymmetric ClO_4 anions at the wave vector $(a/2,b/2,c/2)$.[16] This change in the structural disorder is first order and it is accompanied by a sizeable tetramerization of the organic stack of approximately 0.1 Å.[5] The transition at around 70 K can also be seen in the rocking mode of the methyl groups.[19]

In this paper we present an extensive series of electron spin resonance (ESR) experiments on a large number of TMTCF salts in the normal paramagnetic state as well as in the ordered ground states. The various compounds fully cover the phase diagram (Fig. 1) ranging from quasi-one-dimensional to more two-dimensional systems with a considerable increase of the interchain interaction.

II. EXPERIMENTAL DETAILS

Single crystals of $(TMTTF)_2PF_6$, $(TMTTF)_2ClO_4$, and $(TMTTF)_2Br$ were synthesized electrochemically following a detailed procedure outlined previously.[20] Acetonitrile solutions of TMTTF (0.008 M), $(n\text{-Bu})_4NPF_6$ (0.10 M), and $(n\text{-Bu})_4NClO_4$ (0.025 M) were combined in the prescribed manner, and the electrocrystallizations (platinum electrodes, constant current, 1.5 μA/cm^2) carried out over 10 to 20 day periods. The electrochemical cells were maintained at a constant temperature of 25.0 °C under dry nitrogen in a vibration-isolated environment. The single crystals of the TMTSF salts were grown by the standard electrochemical growth technique.[21]

The electron spin resonance (ESR) experiments were performed in a continuous wave X-band spectrometer (Bruker

Elexsys 500 CW) at 9.5 GHz for temperatures $4 \leqslant T \leqslant 500$ K and magnetic field sweeps from $0 \leqslant H \leqslant 18$ kOe. The modulation frequency was 100 kHz. We use the TE_{102} mode of a rectangular reflection cavity. For cooling the sample down to 4 K, we used a Oxford He-flow cryostat. The sample was glued to a quartz rod by paraffin in order to achieve good thermal contact. The measurements in the temperature range $100 \leqslant T \leqslant 500$ K were performed in a nitrogen gas flow system with the sample embedded in potassium fluoride. Above 500 K the crystals decompose. The single crystals were oriented along their a, b', or c^* axes with an accuracy of $\pm 5°$ by using a microscope.[22]

III. RESULTS

In order to compare the spin and charge degrees of freedom, we first want to summarize the latest results on the transport properties.[23,10] While the Bechgaard salts $(TMTSF)_2X$ with $X = PF_6$, AsF_6, and ClO_4 show metallic conductivity with a monotonic increase of $\sigma(T)$ with decreasing temperature down to T_{SDW},[3] the sulfur analogs exhibit an insulating behavior below $T \approx 200$ K. From photoemission, optical, and dielectric studies,[24,25] gap values of 500–1500 K are estimated in the case of $(TMTTF)_2PF_6$ and 300–400 K in the case of $(TMTTF)_2Br$. The activation energies determined from temperature-dependent transport measurements and the evaluation of Δ_ρ from the minimum resistivity $\Delta_\rho \approx T_\rho \pi \approx 700$ or 300 K, respectively, give values of the same order. Alternatively the conductivity can be described over a wide temperature range by the model of one-dimensional variable-range hopping[26] $\sigma(T) \propto \exp\{-T_0/T^{0.5}\}$. The absolute value of the room-temperature conductivity of $(TMTTF)_2ClO_4$ and $(TMTTF)_2PF_6$ is approximately two orders of magnitude smaller than their selenium counterparts. In $(TMTSF)_2PF_6$ no charge gap develops therefore the material stays metallic down to low temperatures ($T > T_{SDW} = 12$ K), however, indications of $2k_F$ peaks are reported between 20 and 150 K (Ref. 5) which do not lead to long-range order.

The temperature dependence of the ESR results along the three crystal axes of $(TMTTF)_2PF_6$ is shown in Fig. 2. The g shift $\Delta g = g - 2.002\,319$ for all three crystal axes is very small. At temperatures $T > 20$ K, the g values show no significant temperature dependence but a distinct anisotropy with a negative value of Δg along the chain direction a and positive values perpendicular to the chain direction. This behavior is found in all TMTCF salts investigated. The small anisotropy of Δg between the b' and the c^* axis increases with temperature [Fig. 2(c)]. As the temperature is lowered, the linewidth ΔH decreases almost linearly with T in all directions. Around $T = 150$ K a slight and smooth change in slope is observed which can be seen even better in $(TMTSF)_2PF_6$ [Fig. 4(b)].[27] In the c^* direction ΔH is slightly larger; the most narrow lines are always observed along the chains [Figs. 2(b) through 4(b)]. At temperatures $T > 50$ K the intensity of the ESR signal (area under absorption curve) is the same for all three orientations. It exhibits a maximum at around 340 K and continuously drops with decreasing temperature. In the a direction the intensity almost saturates before the phase transition at $T_{SP} = 19$ K as can be seen in Fig. 2(a). For the perpendicular directions b' and c^* the intensity smoothly drops until the temperature reaches the SP transition. Below T_{SP} the intensity rapidly decreases in all directions as expected for a transition to a nonmagnetic ground state, but it does not completely vanish. This phase transition also leads to a broadening of the ESR linewidth and a small change in the g values.

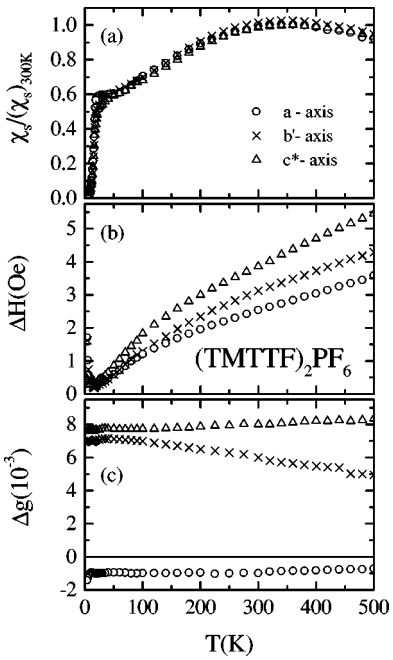

FIG. 2. Temperature dependence of (a) the spin susceptibility as obtained by the ESR intensity, (b) the linewidth ΔH, and (c) the Δg value of $(TMTTF)_2PF_6$ in the three crystal directions.

In the high-temperature range the results of the ESR investigations on $(TMTTF)_2ClO_4$ and $(TMTTF)_2Br$ are similar to the one observed in $(TMTTF)_2PF_6$; even the absolute values of ΔH and g are comparable, as displayed in Fig. 3 for the case of $(TMTTF)_2Br$. Again, the temperature dependence of the ESR intensity exhibits a maximum, with $T_{max} \approx 350$ K in $(TMTTF)_2ClO_4$ and $T_{max} \approx 425$ K in $(TMTTF)_2Br$. At $T_{AO} = 72.5$ K we observe in $(TMTTF)_2ClO_4$ an abrupt change in ΔH and of the intensity in all directions. Although no hysteresis was observed, this jump indicates a first-order phase transition due to the anion ordering.[5] For $T < 70$ K the intensity continues to drop as the temperature is lowered but much faster than in the high-temperature regime; the decrease is exponential with temperature. Below $T = 22$ K the intensity approaches a residual value and even slightly peaks before it suddenly drops at 12 K. Indications of this behavior can be found in Ref. 10. In $(TMTTF)_2Br$, below $T = 17$ K the intensity fully vanishes within a small temperature region, the linewidth increases rapidly and g shifts towards smaller values in b' and c^* direction while it increases in a direction.

The temperature dependence of the ESR results of the Bechgaard salt $(TMTSF)_2PF_6$ is shown in Fig. 4. Above $T_{SDW} = 12$ K the intensity increases almost linearly up to highest temperatures with no indication of saturation. The ESR line is almost 50 times broader and the g shift is five times larger in $(TMTSF)_2PF_6$ than it is in the sulfur analog $(TMTTF)_2PF_6$ (compare Figs. 2 and 4). As seen in Fig. 4(c), at the SDW transition of $(TMTSF)_2PF_6$, we observe an in-

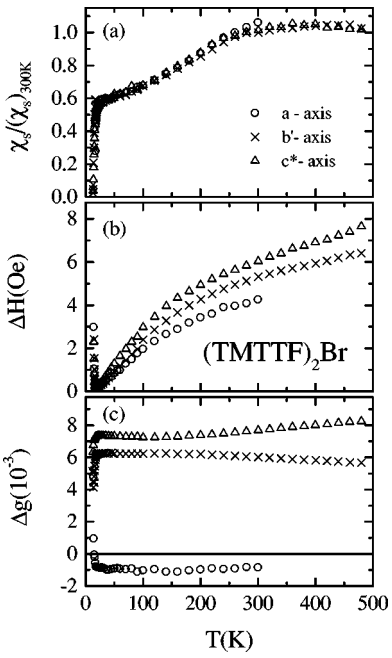

FIG. 3. Temperature dependence of (a) the spin susceptibility as obtained by the ESR intensity, (b) the linewidth ΔH, and (c) the Δg value of $(TMTTF)_2Br$ in the three directions.

crease of Δg along the c^* direction in contrast to the behavior in $(TMTTF)_2Br$. The antiferromagnetic SDW ground state is characterized by an anisotropy of the static susceptibility with b' the easy axis and c^* the hard axis. The signal of the paramagnetic resonance vanishes totally within only 1 K below $T_{SDW}=12$ K. We present only the results on $(TMTSF)_2PF_6$ but a similar behavior was observed in $(TMTSF)_2AsF_6$ and (as far as the room-temperature properties are concerned) in $(TMTSF)_2ReO_4$ and $(TMTSF)_2ClO_4$.

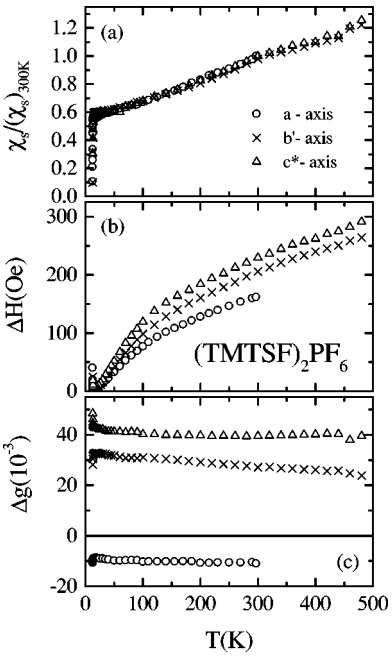

FIG. 4. Temperature dependence of (a) the spin susceptibility as obtained by the ESR intensity, (b) the linewidth ΔH, and (c) the Δg value of $(TMTSF)_2PF_6$ in the three directions.

IV. ANALYSIS AND DISCUSSION

We first want to discuss the normal-state properties for the insulating and metallic compounds before we turn to the ordered ground states (structurally ordered, spin-Peierls, spin-density wave, antiferromagnetically ordered).

A. Paramagnetic state

Going from the left to right side of the phase diagram (Fig. 1), there is a crossover from localized to itinerant charge due to the reduced Coulomb repulsion; the interchain coupling increases making the systems more two dimensional. This should also affect the spin dynamics and lead to insight into the separation of spin and charge degrees of freedom.

1. Spin susceptibility

From a stoichiometric point of view, each TMT*C*F molecule lacks half an electron. Due to the slight dimerization of these compounds the π-electron density is enhanced at the dimers, leading to a deficiency of one electron per TMT*C*F pair. Although the hole density is spread over the dimer, the charge is localized with respect to the chain direction thus forming a localized spin.

The large thermal expansion of the organic compounds certainly has strong effects on the temperature dependence of the spin susceptibility. To compare the experimental results (usually obtained at $p=$const) with the theoretical predictions (in general calculated for $V=$const), the spin susceptibility at constant pressure $(\chi_s)_p$ has to be transformed in the spin susceptibility at constant volume $(\chi_s)_V$. In the case of $(TMTSF)_2PF_6$ the temperature dependence of $(\chi_s)_V$ was estimated by Wzietek *et al.*[14] from NMR and x-ray measurements under pressure. We assumed that the substitution of sulfur for selenium and the exchange of the inorganic anions has no considerable influence on the thermal expansion, thus we took the ratio $(\chi_s)_V/(\chi_s)_p$ for different temperatures to rescale our susceptibility data of $(TMTCF)_2X$ (Fig. 5).

At high temperatures the spin susceptibility at constant volume of $(TMTTF)_2PF_6$ resembles the well-known behavior of a spin-1/2 Heisenberg chain with AFM coupling (Fig. 5). The thermodynamic and magnetic properties of such a system were studied by Bonner and Fisher.[28] The magnetic susceptibility can be fitted numerically[29] by

$$\chi_s(T)=\frac{Ng^2\mu_B^2}{k_BT}\,\frac{0.25+Bx+Cx^2}{1+Dx+Ex^2+Fx^3} \tag{1}$$

with $x=J/T$. In the case of an equally spaced spin chain, the coefficients are given by $B=0.074\,975$, $C=0.075\,235$, $D=0.9931$, $E=0.172\,135$, and $F=0.757\,825$. The advanced EAT model of Eggert, Affleck, and Takahashi[30] using the Bethe ansatz differs significantly only at low temperatures ($T\leqslant 0.2J$). For $T\geqslant 100$ K the ESR intensity at constant volume can be modeled using $J=420$ K. Fitting the temperature in the range of the maximum ESR intensity we directly obtain the absolute value of the spin susceptibility as shown in the figure axis. The deviations below 100 K may be due to interchain coupling. The transfer integral in b direction is

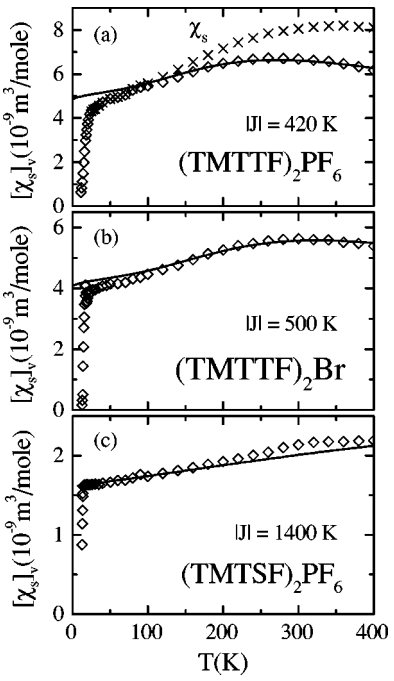

FIG. 5. Temperature dependence of the spin susceptibility at constant volume $(\chi_s)_V$ of (a) $(TMTTF)_2PF_6$, (b) $(TMTTF)_2Br$, and (c) $(TMTSF)_2PF_6$ in b' direction. The lines in (a) and (b) correspond to fits using the EAT model for a $S=1/2$ AFM Heisenberg chain,[30] the line in (c) corresponds to a fit using the model of Seitz and Klein (Ref. 33) with $t_a/U=0.2$.

given by $t_b \approx 150$ K. Near the phase transition $(\chi_s)_V$ is additionally reduced by one-dimensional lattice fluctuations (cf. Sec. IV C 1 below).

The spin susceptibility at constant volume of $(TMTTF)_2ClO_4$ and $(TMTTF)_2Br$ can also be described by the models of Bonner and Fisher[28] or of Eggert *et al.*[30] with $J=430$ K (ClO_4) and $J=500$ K (Br) for $T \geqslant 100$ K. In the high-temperature region, all $(TMTTF)_2X$ compounds investigated behave like $S=1/2$ antiferromagnetic Heisenberg chains with localized spins. This findings are in contrast to the results of the transport measurements, which show a transition from semiconducting to metallic behavior around 100–300 K. No sign of the resistivity minimum can be found in the spin dynamics implying a decoupling of the spin and charge degrees of freedom as expected for a one-dimensional system.[31,32]

The steady increase of the spin susceptibility with increasing temperature in the metallic TMTSF salts (Fig. 4) is in contradiction to a temperature-independent paramagnetic term as expected for a simple metal. It may resemble the increase of the density of states with temperature. In the lower part of Fig. 5 $(\chi_s)_V$ of the selenium compound $(TMTSF)_2PF_6$ is plotted versus temperature. Comparing $(\chi_s)_V$ with the spin susceptibility at constant pressure $(\chi_s)_p$ the elimination of the effects of thermal expansion leads to a weaker temperature dependence of the spin susceptibility. Within the framework of the Hubbard-model this behavior can neither be described by an enhanced Pauli susceptibility as expected for a one-dimensional metal in the limit of weak coupling ($t_a \gg U$) nor by a $S=1/2$ antiferromagnetic Heisenberg chains with localized spins ($t_a \ll U$). This is not surprising since the transfer integral along the a axis is $t_a = 231$ meV and the on-site Coulomb repulsion $U = 1.16$ eV,[14] leading to $t_a/U \approx 0.25$. The models of a $S=1/2$ spin chain only describe the behavior of one-dimensional electronic systems in the high U limit and therefore are not appropriate for $(TMTSF)_2PF_6$.

Going beyond the strictly localized models, Seitz and Klein calculated the temperature dependence of the spin susceptibility in a linear half filled Hubbard model for different values of the Coulomb repulsion $t_a/U=0$, 0.05, 0.1, 0.15, and 0.2.[33] In the atomic limit $t_a/U=0$ χ_s resembles the behavior of a $S=1/2$ antiferromagnetic Heisenberg chain; for $t_a/U \geqslant 0.1$ the maximum in χ_s/J is shifted towards lower values of T/J. The temperature dependence of the spin susceptibility at constant volume of $(TMTSF)_2PF_6$ was fitted by the model of Seitz and Klein with $t_a/U=0.2$ and $J=1400$ K. The remaining deviations between model and experiment can be explained by the fact that Seitz and Klein calculated the spin susceptibility only in the limit of a rather strong Coulomb repulsion $t_a/U \leqslant 0.2$ and not in the case of $t_a/U=0.25$ as appropriate in our case. Even though the Bechgaard salts are one-dimensional organic metals down to low temperatures the magnetic properties of these compounds can be explained in the framework of the Hubbard model in the limit of strong electronic correlations.

It is interesting to note that despite the fact that the TMTSF and TMTTF salts exhibit distinctively different electronic properties and even at room temperature the conductivity is more than an order of magnitude different, the absolute values of the spin susceptibility of all compounds are similar within a factor of 3 in the whole temperature range. The stronger localization of the charge carriers in the sulfur compounds leads to a moderate increase of the spin susceptibility. In the Introduction we pointed out that the opening of a charge gap Δ_ρ due to increased Coulomb interaction and dimerization is accompanied by a drastic increase of the resistivity in these materials. While the ESR signal of the conduction electrons is observed in the one-dimensional organic metal $(TMTSF)_2PF_6$, the TMTTF compounds are insulating. The minimum in resistivity found in $(TMTTF)_2PF_6$ and $(TMTTF)_2ClO_4$ at approximately 230 K does not show up in any of the ESR results. This indicates that no drastic change of the physical properties takes place, like a metal-insulator phase transition. Instead the change from an itinerant charge to a Mott-Hubbard localization is due to a gradual increase of the dimerization as observed by studies of the vibronic features.[19] The fact of a crossover from metallic to insulating behavior while the spin degrees of freedom remain gapless is evidence of spin-charge separation. This behavior is predicted by the Tomonaga-Luttinger theory for a one-dimensional interacting electron system.[31,32] Indications for the separation of spin and charge are also seen by photoemission spectroscopy.[24] Furthermore, these experiments do not show a sharp edge in the spectral function at the Fermi energy as required by the Fermi-liquid theory.[34] The experimental results on the organic linear chain compounds are in accord with observations on inorganic one-dimensional systems like $SrCuO_4$.[35]

2. Linewidth and g shift

The temperature dependences of the linewidth ΔH and the g shift Δg of $(TMTTF)_2PF_6$, $(TMTTF)_2Br$, and

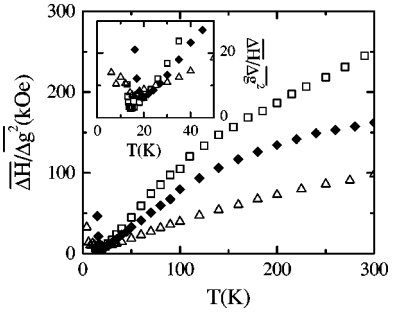

FIG. 6. Temperature dependence of the reduced linewidth $\Delta H_{\rm red}=\overline{\Delta H}/\overline{\Delta g^2}$ of $(TMTSF)_2PF_6$ (□), $(TMTTF)_2Br$ (◇), and $(TMTTF)_2PF_6$ (△). The data are *not* normalized. The inset shows an enlarged view of the low-temperature range.

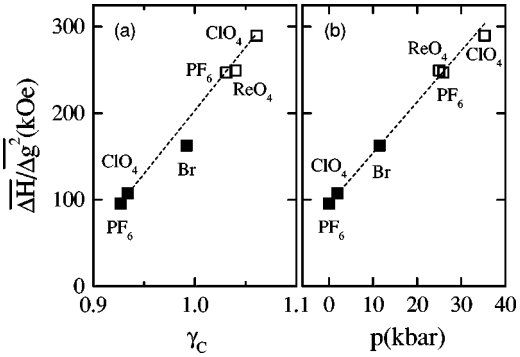

FIG. 7. Reduced linewidth $\overline{\Delta H}/\overline{\Delta g^2}$ of $(TMTTF)_2X$ (closed symbols) and $(TMTSF)_2X$ (open symbols) at $T=300$ K. For $(TMTSF)_2AsF_6$ and $(TMTSF)_2PF_6$ the points are virtually identical.

$(TMTSF)_2PF_6$ are shown in the second and third panels of Figs. 2, 3, and 4, respectively. All materials investigated in this work are characterized by a distinct anisotropy in both quantities. It is obvious, that the ESR linewidth has the same angular dependence as the g value. This is a strong indication for spin-phonon interaction as the dominant scattering process. In this case, the spin-phonon coupling is proportional to the mean value of the squares of the g shifts in three crystal directions $\overline{\Delta g^2}=(\Delta g_a^2+\Delta g_{b'}^2+\Delta g_{c*}^2)/3$.[7] Due to the much stronger spin-phonon coupling in selenium the g shift increases about five times if sulfur is replaced by selenium.

To compare the linewidth of $(TMTTF)_2X$ and $(TMTSF)_2X$ the effects of the stronger spin-orbit coupling in selenium have to be considered. As mentioned above, $\overline{\Delta g^2}$ is a measure of the spin-orbit coupling and therefore the reduced linewidth $\Delta H_{\rm red}=\overline{\Delta H}/\overline{\Delta g^2}$ is the suitable quantity for comparison, where $\overline{\Delta H}=(\Delta H_a+\Delta H_{b'}+\Delta H_{c*})/3$. Figure 6 shows the temperature dependence of $\Delta H_{\rm red}$ of $(TMTTF)_2PF_6$, $(TMTTF)_2Br$, and $(TMTSF)_2PF_6$. Right above the phase transition the reduced linewidth reaches nearly the same value in all three materials. Towards higher temperatures $\Delta H_{\rm red}$ increases most strongly in $(TMTSF)_2PF_6$, followed by $(TMTTF)_2Br$ and $(TMTTF)_2PF_6$. For all TMT*C*F compounds we find a kink in the temperature-dependent linewidth at around 150 K which we feel is not related to the crossover from one- to two-dimensional behavior which happens at around this temperature. Instead it might be relevant that the Debye temperature is about in this temperature range.

The linewidth ΔH of the quasi-one-dimensional conductor $(TMTSF)_2PF_6$ shows a similar value and temperature dependence in all three directions [Fig. 4(b)]. This behavior is in contrast to the large anisotropy and distinctively different temperature dependence reported for the dc resistivity.[36,37] If spin-phonon coupling is the dominant relaxation process in quasi-one-dimensional conductors, the reduced linewidth becomes proportional to the relaxation rate of tunneling processes between chains $1/\tau_\perp$,[38]

$$\Delta H/\Delta g^2 \propto 1/\tau_\perp , \tag{2}$$

and is therefore a measure of the interchain couplings. Equation (2) is an expansion of the well-known Elliott formula[39] which is only valid in the case of isotropic three-dimensional metallic transport. The increase of the reduced linewidth from $(TMTTF)_2PF_6$ over $(TMTTF)_2Br$ to $(TMTSF)_2PF_6$ is an indication of the increasing interchain coupling. Flandrois *et al.*[7] pointed out that the reduced linewidth increases linearly with the ratio γ_C between twice the van der Waals radius of S or Se and the shortest interstack distances between the chalcogen atoms. The numerical values of γ_C are listed in Table I. The left side of Fig. 7 shows the room-temperature value $\overline{\Delta H}/\overline{\Delta g^2}$ versus γ_C of all compounds investigated including $(TMTSF)_2ReO_4$ and $(TMTSF)_2ClO_4$. Indeed, there is a linear increase of the reduced linewidth with γ_C which proves that $\Delta H_{\rm red}$ is a measure of the interaction between the molecular stacks.

For each member of the $(TMTCF)_2X$ family the reduced linewidth can now be plotted as a function of pressure as determined from the phase diagram (Fig. 1); the room-temperature result is shown on the right side of Fig. 7. The reduced linewidth and therefore the interchain coupling increases linearly with pressure. $(TMTTF)_2ClO_4$ was included in the diagram at $p=2$ kbars by means of its reduced linewidth.

B. Ordered states

Upon lowering the temperature the TMT*C*F salts undergo transitions to different ground states. In $(TMTTF)_2ClO_4$ the anion ordering is the driving force of the development of a crystallographic superstructure (tetramerization). The spin-Peierls transition in $(TMTTF)_2PF_6$ is also accompanied by a structural change, but driven by spin-phonon coupling, leading to a nonmagnetic ground state. The antiferromagnetic ground states of $(TMTTF)_2Br$ and $(TMTSF)_2PF_6$ are due to the ordering of the electronic and spin system with the coupling to the lattice being negligible.[40]

1. Structural phase transition in $(TMTTF)_2ClO_4$

The alternating order of the ClO_4^- anions in a $q_{\rm AO}=(1/2,1/2,1/2)$ superstructure at $T_{\rm AO}\approx 72.5$ K leads to a doubling of the unit cell in $(TMTTF)_2ClO_4$. This first-order phase transition is accompanied by a steplike decrease in the ESR intensity and increase in the linewidth as the temperature is lowered through $T_{\rm AO}$. The sudden decrease of the electrical resistivity indicates the scattering to be reduced in

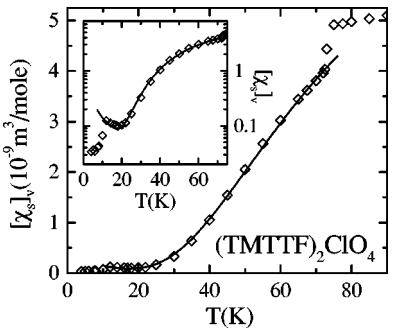

FIG. 8. Low-temperature behavior of the spin susceptibility of $(TMTTF)_2ClO_4$ along the b' directions. The decreasing intensity below $T_{AO}=72.5$ K can be well described by Bulaevskii's model (Ref. 41) of an alternating spin chain with $\gamma=0.79$ and a singlet-triplet gap $\Delta_\sigma(0)=84.5$ K (line). The inset shows the same data on a logarithmic scale in order to stress the saturation of the signal below 22 K and the second transition at 12 K.

the ordered state and rules out a change in the density of states due to the formation of a pseudogap.

Figure 8 shows the spin susceptibility at constant volume of $(TMTTF)_2ClO_4$ for $T\leqslant 90$ K. Below the first-order phase transition at T_{AO} the intensity drops exponentially due to the tetramerization of the TMTTF stacks. Using the result which Bulaevskii[41] obtained from a Hartree-Fock approximation in the case of an alternated one-dimensional AFM Heisenberg chain with $S=1/2$, $\chi_s(T)$ below T_{AO} is given by

$$\chi_s(T)=\frac{\alpha}{T}\exp\left[-\frac{J_1\beta}{T}\right]. \tag{3}$$

α and β are tabulated in Ref. 41 for given values of the alternation parameter $\gamma=[1-\delta]/[1+\delta]=J_2/J_1$; $J_{1,2}=J[1\pm\delta]$ are the exchange integrals of the weakly dimerized chain. An additional Curie contribution $\chi_c=C/T$, $C=1.4\times10^{-9}$ m^3 K/mole, is needed to describe the slight increase of the susceptibility at low temperatures. For the fit parameters $J_1\beta=173$ K and $J=430$ K we obtain $\gamma=0.79$, $J_1=482$ K, and $J_2=378$ K. The temperature-independent singlet-triplet gap is given by $\Delta_\sigma=1.637\delta J=84.5$ K. Since Bulaevskii's model assumes $\delta=$const at any temperature, it fits the data of $(TMTTF)_2ClO_4$ up to higher values of T/T_c compared to the second-order phase transition in $(TMTTF)_2PF_6$ (see Sec. IV B 2 below).

The inset of Fig. 8 magnifies the intensity in the low-temperature region. The signal passes through a minimum at around 20 K and then increases until 12 K. Below 12 K the intensity drops nearly by one decade. In addition as the temperature goes below 15 K, the ESR signal changes its shape significantly in all three crystal directions: it consists of a small central resonance line and five additional lines with a strong angular dependence. This effect increases as the temperature approaches 12 K, however at lower temperatures the intensity of the five additional lines decreases rapidly, while the intensity of the small central line is nearly temperature independent. The splitting of the lines which is about 5 Oe can be explained by hyperfine interaction between the electron spins and the nuclear spins of hydrogen atoms of the methyl groups. It is known from ^{1}H-NMR experiments that the methyl groups which rotate at high temperatures slow down below 20 K,[42] thus the rotational narrowing causes the temperature dependence of the hyperfine splitting. The drastic decrease of the spin susceptibility below 12 K may be due to a more perfect ordering of the anions, which is induced by the freezing of the rotational degrees of freedom of the methyl groups. The drop of χ_s is accompanied by an increase of ΔH, which can be interpreted as a critical behavior above an antiferromagnetic phase transition, thus there are two possible explanations for the decrease of the susceptibility below 12 K.

2. Spin-Peierls state in $(TMTTF)_2PF_6$

For energetic reasons the electrons in a one-dimensional spin system with antiferromagnetic interaction tend to form singlet pairs by alternating the spacing between them. As a result, at low temperature the SP state accompanied by a lattice modulation may become more stable than the antiferromagnetically ordered state with regular chains. The formation of states with singlet-paired holes due to the tetramerization causes a decreasing susceptibility with an exponential drop of the intensity down to lowest temperatures. This is in contrast to the SDW phase transition, like in $(TMTSF)_2PF_6$, where due to the opening of an energy gap at the Fermi surface the density of the conduction electrons decreases at the transition causing a sudden change in resistivity and in the susceptibility as can be seen in Fig. 4(a). The decrease of the ESR intensity in the case of a SDW is much more rapid than the drop observed at a SP transition.

We can describe the temperature-dependent susceptibility by Bulaevskii's formula (3). Originally this model assumed a temperature-independent alternation δ and the extension to a second-order phase transition, like a spin-Peierls phase, breaks down close to T_{SP}. The temperature dependence of the singlet-triplet gap $\Delta_\sigma(T)$ can be described by mean-field theory and yields a BCS-like behavior. The order parameter is related to the alternation via $\delta(T)=\Delta_\sigma(T)/(1.637J)$ which now is assumed to be temperature dependent[43] and $\gamma(T)=[1-\delta(T)]/[1+\delta(T)]=J_2(T)/J_1(T)$. For $T\ll T_{SP}$, δ is nearly temperature independent, thus the ESR intensity can be fitted as a alternating spin chain with the dimerization to be temperature independent.

At the SP transition a smooth increase of $\Delta H(T)$ with falling T corresponds to the drop of the ESR intensity, indicating additional scattering effects due to the rearrangement of the lattice. We observe a slight increase of the g value along the chain direction at $T_{SP}=19$ K while in the directions perpendicular to the stacks the g value decreases [Fig. 2(c)].

In Fig. 9 the low-temperature behavior of the spin susceptibility measured on $(TMTTF)_2PF_6$ is displayed. Up to 12 K the data can be fitted by Eq. (3) after substituting the numerator of the exponential function $J_1\beta(\gamma)$ by $J[1+\delta(\gamma)]\beta(\gamma)=J\beta'(\gamma)$. Using the exchange energy $J=420$ K from the Bonner-Fisher fit we obtain $\gamma=0.91$ for the alternation parameter of the dimerized spin chain, yielding to $J_1=440$ K and $J_2=400$ K. From our fits of the data in all three directions we find almost identical values of the singlet-triplet gap of $(TMTTF)_2PF_6$: $\Delta_\sigma=32.3$ K in the $T=0$ limit.

There is an excellent agreement of $2\Delta_\sigma(0)/T_{SP}=3.4$ with the value of 3.53 predicted by the mean-field theory. This

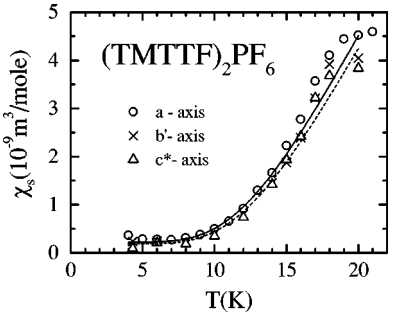

FIG. 9. Low-temperature behavior of the spin susceptibility of $(TMTTF)_2PF_6$. At $T_{SP}=19$ K the intensity drops in all three directions indicating the spin-Peierls transition to a nonmagnetic ground state. The lines corresponds to fits using Eq. (3) with different parameters appropriate for the different orientations.

agreement can be explained by the fact that in the spin-Peierls state the quasi-one-dimensional electronic system is coupled to a three-dimensional lattice and that fluctuation effects can be neglected well below the transition temperature. Both, the classical organic spin-Peierls system MEM-$(TCNQ)_2$ (Ref. 44) and the recently discovered inorganic compound $CuGeO_3$ (Ref. 45) show a quite similar behavior below T_{SP}. The temperature dependence of the spin susceptibility and the magnetic gap $\Delta_\sigma(0)$ of the materials can be explained within the mean-field theory.

3. Spin-density-wave ground state in $(TMTSF)_2PF_6$

In the SDW ground state, the static susceptibility of the Bechgaard salts exhibits the behavior typically expected for an antiferromagnet.[46] Along the b' direction, $\chi_s(T)$ drops rapidly when the temperature is lowered through T_{SDW} as expected for the easy axis; the hard and intermediate axes are along c^* and a, respectively. In agreement with these findings, the ESR line of the conduction electrons in $(TMTSF)_2PF_6$ dramatically broadens and shifts in field upon passing through the phase transition at $T_{SDW}=12$ K (Fig. 4), indicating the development of internal magnetic fields. The signal fully vanishes within a temperature interval of 1 K in all three directions; no fluctuation effects are observed in $\chi_s(T)$. All the carriers and thus all the spins enter a collective state, in which the spins form pairs; this behavior can serve as evidence for the development of a spin-density wave.

As the temperature decreases further one or two other resonance lines are observed depending on the orientations of the crystal with respect to the static and microwave fields. Since they are significantly smaller in intensity and well separated in magnetic field from the original ESR signal, they can unambiguously be identified as antiferromagnetic resonances.[47]

The three-dimensional ordering is due to interaction of the spins in the transverse direction through an interchain exchange interaction $J_\perp$. As pointed out by Bourbonnais[48] this coupling involves the coherent propagation of electron-hole pairs perpendicular to the chains although no coherent charge transport is possible.

4. Antiferromagnetic ground state in $(TMTTF)_2Br$

In contrast to the SDW ground state of $(TMTSF)_2PF_6$, in $(TMTTF)_2Br$ the antiferromagnetic phase transition is induced by a three-dimensional ordering of the one-dimensional chains of localized spins. The interchain exchange $J_\perp$ gives rise to a finite coupling between the chains. Following Ogushi,[49] from the transition temperature $T_N=13.3$ K the ratio between the interchain and intrachain coupling can be estimated with $J_\perp/J\approx 0.001$, i.e., $J_\perp\approx 0.5$ K.

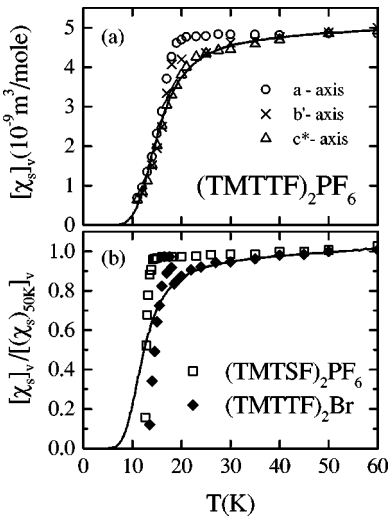

FIG. 10. Temperature dependence of $(\chi_s)_V$ of $(TMTTF)_2PF_6$ (a) and $(TMTTF)_2Br$ or $(TMTSF)_2PF_6$, respectively, in b' direction (b) near the phase transitions. The lines represent fits using a model for one-dimensional lattice fluctuations in the spin-Peierls pseudogap regime (Ref. 51) below a characteristic temperature $T_{SP}^0=62$ K $[(TMTTF)_2PF_6]$ and $T_{SP}^0=50$ K $[(TMTTF)_2Br]$.

The magnetic anisotropy of the antiferromagnetic ground state of the sulfur compounds differs from that of the selenium compounds: the hard axis is orientated along the a direction and the intermediate axis along the c^* direction, while the easy axis is as well orientated in the b' direction. The change in the anisotropy can be explained by stronger effects of the spin-orbit coupling in $(TMTSF)_2X$ which favor the a direction.[50] Above T_N, the ESR signal vanishes within a temperature interval of 4 K in all three directions. Below T_N, again we observe antiferromagnetic resonances with its characteristic angular dependences.

C. Fluctuations

1. One-dimensional lattice fluctuations

Above the spin-Peierls transition there is a distinct decrease in the spin susceptibility of $(TMTTF)_2PF_6$ for temperatures $T\leqslant 60$ K in b' and c^* direction [Fig. 10(a)] whereas $(\chi_s)_V$ is nearly temperature-independent in a direction. A reduced spin susceptibility is expected[51] if one-dimensional lattice fluctuations are present in the temperature region above a second-order phase transition. Below the characteristic temperature T_{SP}^0 the lattice fluctuations lead to a decrease of the density of states and therefore of the spin susceptibility. The data in b' and c^* directions are fitted by Bourbonnais' model for one-dimensional spin-Peierls fluctuations[51] which predict a specific temperature dependence. We determined a characteristic temperature $T_{SP}^0=62$ K. These results are in agreement with previous x-ray,

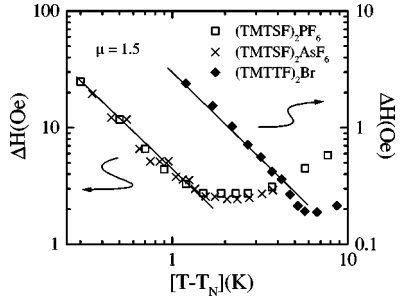

FIG. 11. Double-logarithmic plot of the linewidth ΔH vs $T-T_N$ of $(TMTSF)_2PF_6$ and $(TMTSF)_2AsF_6$ (left axis) and $(TMTTF)_2Br$ (right axis) near the antiferromagnetic phase transitions in b' direction. The lines represent a slope $\mu=1.5$. $T_N=12$ K in the case of $(TMTSF)_2PF_6$ and $(TMTSF)_2AsF_6$ and $T_N=13.3$ K for $(TMTTF)_2Br$.

^{13}C NMR and ESR investigations.[16,17] The anisotropy of the lattice fluctuations may be due to the influence of the static magnetic field H, $H_{res}\approx 3.48$ kOe. If the field is applied along the a axis the spins are aligned parallel to H which could suppress the fluctuations. The ^{13}C NMR and ESR measurements of Creuzet *et al.* were discussed for different orientations and thus do not yield any angular dependence.

Recently Pouget *et al.* also observed one-dimensional lattice fluctuations in $(TMTTF)_2Br$ (Ref. 52) which passes through an antiferromagnetic phase transition at $T_N\approx 13$ K. Figure 10(b) shows the spin susceptibility at constant volume of $(TMTTF)_2Br$ and $(TMTSF)_2PF_6$ in the b' direction normalized at 50 K. In the selenium compound there is only a weak temperature dependence of $(\chi_s)_V$ above the AFM phase transition and then the ESR signal vanishes completely within a temperature interval $\Delta T=1$ K. In contrast, the spin susceptibility of $(TMTTF)_2Br$ decreases significantly in all crystal directions for decreasing temperatures below 50 K. At $T=19$ K there is a sharp increase of the ESR intensity, afterwards the signal vanishes almost completely within $\Delta T\approx 4$ K. Between $19\leqslant T\leqslant 50$ K the temperature dependence of $(\chi_s)_V$ can be fitted by the model for one-dimensional spin-Peierls fluctuations. This complicated behavior can be interpreted in the following way: below a characteristic temperature $T_{SP}^0=50$ K the one-dimensional lattice fluctuations give rise to a reduced spin susceptibility. In the close vicinity of the AFM phase transition these fluctuations collapse and $(\chi_s)_V$ increases suddenly. Our findings are in accordance with the x-ray investigations of Pouget *et al.* who detected lattice distortions in $(TMTTF)_2Br$ at $q=2k_F$ below $T=70$ K. The spin-Peierls response function does not reach the critical value as in $(TMTTF)_2PF_6$ and vanishes below $T=20$ K.

2. Antiferromagnetic fluctuations

In $(TMTTF)_2Br$, $(TMTSF)_2PF_6$, and $(TMTSF)_2AsF_6$ there is a distinct increase of the linewidth near the antiferromagnetic phase transitions. As seen in Fig. 11 this temperature dependence of ΔH follows a critical behavior; previous ESR investigations of $(TMTSF)_2PF_6$ led to similar observations.[53] The singularity of the linewidth can be explained by three-dimensional antiferromagnetic fluctuations in the vicinity of a phase transition. In the case of a small static magnetic field H the linewidth is given by

$$\Delta H(T>T_N)=C\left(\frac{T-T_N}{T_N}\right)^{-\mu}, \tag{4}$$

where C is a constant. The parameter μ is a function of the critical indices and the dimension d; it is given by $\mu=3-d/2$ in the case of dipole-dipole interactions, e.g., $\mu=1.5$ for $d=3$.[48] A good fit of the divergent ESR linewidth observed in our experiments is achieved for $\mu=1.5$ in all three compounds, indicating three-dimensional AFM fluctuations near the phase transition. These results of the ESR measurements confirm NMR measurements on $(TMTSF)_2PF_6$ (Ref. 54) and $(TMTTF)_2Br$,[55] where a critical divergence in the relaxation rate $1/T_1$ was found above the antiferromagnetic phase transitions.

In $(TMTTF)_2Br$ the angular dependence of the linewidth changes in the regime of the antiferromagnetic fluctuations. At high temperatures where the spin-phonon interaction is the dominant relaxation process, ΔH has the same angular dependence as the g value with $\Delta H_a<\Delta H_{b'}<\Delta H_{c*}$ (Fig. 3), whereas in the temperature region right above the phase transition at $T_N\approx 13$ K the broadest lines are measured along the a direction and the smallest lines in the a-b' plane at $\theta\approx 55°$. This minimum in the linewidth near the magic angle $\theta\approx 54.7°$ is characteristic for dipole-dipole interaction as the dominant relaxation process. No change of the angular dependence of linewidth is observed in the selenium salts. This behavior indicates the change in the anisotropy of the different antiferromagnetic ground states when selenium is exchanged by sulfur.

V. CONCLUSION

We have performed a comprehensive study of the spin dynamics of the organic linear chain compounds $(TMTTF)_2PF_6$, $(TMTTF)_2ClO_4$, $(TMTTF)_2Br$, $(TMTSF)_2PF_6$, and $(TMTSF)_2AsF_6$ by X-band ESR experiments on single crystals in the temperature range from 4 to 500 K. After eliminating the effects of thermal expansion, at high temperatures the spin susceptibility of the $(TMTTF)_2X$ compounds can be described by a spin-1/2 antiferromagnetic Heisenberg chain with exchange constants $J=420$ K ($X=PF_6$), $J=430$ K ($X=ClO_4$), and $J=500$ K ($X=Br$). Even though $(TMTSF)_2PF_6$ and $(TMTSF)_2AsF_6$ are one-dimensional organic metals down to low temperatures, for $T>100$ K the temperature dependence of the spin susceptibility can be described within the framework of the Hubbard model in the limit of strong Coulomb repulsion with $J\approx 1400$ K. Going from the fully insulating $(TMTTF)_2PF_6$ to the highly metallic $(TMTSF)_2PF_6$ there is an sudden change in the charge-transport properties when the transfer integral becomes comparable to the charge gap, while the spin dynamics changes continuously described by a steadily increasing exchange constant. This behavior indicates the separation of spin and charge degrees of freedom.

$(TMTTF)_2ClO_4$ and $(TMTTF)_2PF_6$ undergo a phase transition with a structural change leading to a tetramerization of the chains. The spin-Peierls transition in $(TMTTF)_2PF_6$ at $T_{SP}=19$ K leads to a smaller singlet-triplet gap $\Delta_\sigma=32.3$ K than the anion ordering in $(TMTTF)_2ClO_4$ at $T_{AO}=72.5$ K with $\Delta_\sigma=84.5$ K. In $(TMTTF)_2ClO_4$ we find indications of an additional transi-

tion at around 12 K which may be due to long-range three-dimensional ordering. Above the phase transitions the magnetic behavior of the investigated materials is characterized by fluctuation effects. In $(TMTTF)_2Br$ we found one-dimensional lattice fluctuations below $T_{SP}^0 = 50$ K which break down in the same temperature region where the three-dimensional antiferromagnetic fluctuations occur.

In the high-temperature region the ESR linewidth ΔH is dominated by spin-phonon interactions. We found a linear increase of the reduced linewidth $\overline{\Delta H}/\overline{\Delta g^2}$ from $(TMTTF)_2PF_6$ over $(TMTTF)_2Br$ to $(TMTSF)_2ClO_4$ which scales almost perfectly with the increase of the chemical pressure and the interactions between the molecular stacks. The higher value of $\overline{\Delta H}/\overline{\Delta g^2}$ in $(TMTSF)_2X$ proves the more two-dimensional character of these compounds.

ACKNOWLEDGMENTS

We thank C. Bourbonnais, W. G. Clark, and H.-A. Krug von Nidda for useful discussions. The work at Augsburg was supported by the BMBF under Contract No. EKM 13N6917. The crystal growth at Bloomington was supported by the Division of Material Research of the National Science Foundation (Grant No. DMR-9414268).

[1] M. Hase, I. Terasaki, and K. Uchinokura, Phys. Rev. Lett. **70**, 3651 (1993); for a recent review, see J. P. Boucher and L. P. Regnault, J. Phys. I **6**, 1939 (1996).

[2] M. Isobe and Y. Ueda, J. Phys. Soc. Jpn. **65**, 1178 (1996).

[3] D. Jérome and H. J. Schulz, Adv. Phys. **31**, 299 (1982); T. Ishiguro, K. Yamaji, and G. Saito, in *Organic Superconductors*, 2nd ed., Springer Series in Solid-State Sciences Vol. 88 (Springer-Verlag, Berlin, 1998); *Organic Conductors*, edited by J. P. Farges (Marcel Dekker, New York, 1994); C. Bourbonnais and D. Jérome, cond-mat/9903101 (unpublished).

[4] J. Moser, M. Gabay, P. Auban-Senzier, D. Jérome, K. Bechgaard, and J. M. Fabre, Eur. Phys. J. B **1**, 39 (1998).

[5] J. P. Pouget and S. Ravy, J. Phys. I **6**, 1501 (1996).

[6] L. Ducasse, M. Abderrabba, J. Hoarau, M. Pesquer, B. Gallois, and J. Gaultier, J. Phys. C **19**, 3805 (1986); L. Ducasse, M. Abderrabba, B. Gallois, and D. Chasseau, Synth. Met. **19**, 327 (1987).

[7] S. Flandrois, C. Coulon, P. Delhaes, D. Chasseau, C. Hauw, J. Gaultier, J. M. Fabre, and L. Giral, Mol. Cryst. Liq. Cryst. **79**, 307 (1982).

[8] B. Liautard, S. Peytavin, G. Brun, and M. Maurin, J. Phys. Colloq. **44**, C3-951 (1983).

[9] P. Delhaes, C. Coulon, J. Amiell, S. Flandrois, E. Toreilles, J. M. Fabre, and L. Giral, Mol. Cryst. Liq. Cryst. **50**, 43 (1979).

[10] C. Coulon, P. Delhaes, S. Flandrois, R. Lagnier, E. Bonjour, and J. M. Fabre, J. Phys. (France) **43**, 1059 (1982).

[11] V. Emery, R. Bruisma, and S. Barisic, Phys. Rev. Lett. **48**, 1039 (1982). An alternative explanation interprets the resistivity minimum by a competition between the mobility which decreases with T and the number of charge carriers excited across an energy gap which increases with T. See, for example, Ref. 3.

[12] K. Penc and F. Mila, J. Phys. IV **3**, C2-155 (1993); Phys. Rev. B **50**, 11 429 (1994).

[13] F. Creuzet, Mol. Cryst. Liq. Cryst. **119**, 289 (1985).

[14] P. Wzietek, F. Creuzet, C. Bourbonnais, D. Jérome, K. Bechgaard, and P. Batail, J. Phys. I **3**, 171 (1993).

[15] S. S. P. Parkin, J. C. Scott, J. B. Torrance, and E. H. Engler, J. Phys. Colloq. **44**, C3-1111 (1983).

[16] J. P. Pouget, R. Comes, K. Bechgaard, J. M. Fabre, and L. Giral, Physica B **108**, 1197 (1981); J. P. Pouget, R. Comes, K. Bechgaard, J. M. Fabre, and L. Giral, Mol. Cryst. Liq. Cryst. **79**, 129 (1982).

[17] F. Creuzet, C. Bourbonnais, L. G. Caron, and K. Bechgaard, Synth. Met. **19**, 289 (1987).

[18] The upturn at the lowest temperature seems to be uncertain (Refs. 10 and 7).

[19] R. Bozio, M. Meneghetti, and C. Pecile, J. Chem. Phys. **76**, 5785 (1982).

[20] L. K. Montgomery, in *Organic Conductors*, edited by J. P. Farges (Marcel Dekker, New York, 1994), p. 138ff.

[21] K. Bechgaard, C. S. Jacobsen, K. Mortensen, H. J. Pedersen, and N. Thorup, Solid State Commun. **33**, 1119 (1980).

[22] The TMT*C*F salts have a triclinic crystal structure; however, the angles are close to 90°. The b' direction is normal to the a axis, c^* is normal to the ab plane.

[23] J. Hemberger, M. Dumm, M. Dressel, and L. Montgomery (unpublished).

[24] F. Zwick, D. Jérome, G. Margaritondo, M. Onellion, J. Voit, and M. Grioni, Phys. Rev. Lett. **81**, 2974 (1998).

[25] V. Vescoli, L. Degiorgi, W. Henderson, G. Grüner, K. P. Starkey, and L. K. Montgomery, Science **281**, 1181 (1998).

[26] N. F. Mott and E. A. Davies, *Electronic Processes in Non-Crystalline Materials* (Oxford University Press, Oxford, 1979).

[27] It is interesting to note that a similar change in slope is also observed in the quasi-one-dimensional inorganic SP compound α'-NaV_2O_5. J. Hemberger, M. Lohmann, M. Nicklas, A. Loidl, M. Klemm, G. Obermeier, and S. Horn, Europhys. Lett. **42**, 661 (1998).

[28] J. C. Bonner and M. E. Fisher, Phys. Rev. **135**, A640 (1964).

[29] W. E. Estes, D. P. Gavel, W. E. Hatfield, and D. Hodgson, Inorg. Chem. **17**, 1415 (1978).

[30] S. Eggert, I. Affleck, and M. Takahashi, Phys. Rev. Lett. **73**, 332 (1994).

[31] H. J. Schulz, Int. J. Mod. Phys. B **5**, 57 (1991).

[32] J. Voit, Rep. Prog. Phys. **57**, 977 (1994).

[33] W. A. Seitz and D. J. Klein, Phys. Rev. B **9**, 2159 (1974).

[34] B. Dardel, D. Malterre, M. Grioni, P. Weibel, Y. Baer, J. Voit, and D. Jérome, Europhys. Lett. **24**, 687 (1993); F. Zwick, S. Brown, G. Margaritondo, C. Merlic, M. Onellion, J. Voit, and M. Grioni, Phys. Rev. Lett. **79**, 3982 (1997).

[35] C. Kim, A. Y. Matsuura, Z.-X. Shen, N. Motoyama, H. Eisaki, S. Uchida, T. Tohyama, and S. Maekawa, Phys. Rev. Lett. **77**, 4054 (1996).

[36] C. S. Jacobsen, D. B. Tanner, and K. Bechgaard, Phys. Rev. Lett. **46**, 1142 (1981).

[37] F. Zámborszky, G. Szeghy, G. Abdussalam, L. Forró, and G. Mihály, Phys. Rev. B **60**, 4414 (1999).

[38] S. Shitzkovsky, M. Weger, and H. Gutfreund, J. Phys. (Paris) **39**, 711 (1978).

[39] R. J. Elliott, Phys. Rev. **96**, 266 (1954).
[40] A small influence on the lattice is detected by x-ray scattering (Ref. 5) and acoustic experiments: S. Zherlitsyn, G. Bruls, A. Goltsev, B. Alavi, and M. Dressel, Phys. Rev. B **59**, 13 861 (1999).
[41] L. N. Bulaevskii, Fiz. Tverd. Tela (Leningrad) **11**, 1132 (1969) [Sov. Phys. Solid State **11**, 921 (1969)].
[42] C. J. Schott, E. M. Engler, W. G. Clark, C. Murayama, K. Bechgaard, and H. J. Pederson, Mol. Cryst. Liq. Cryst. **79**, 417 (1982).
[43] E. Pytte, Phys. Rev. B **10**, 4637 (1974).
[44] S. Huizinga, J. Kommandeur, G. A. Sawatzky, B. T. Thole, K. Kopinga, W. J. M. de Jonge, and J. Roos, Phys. Rev. B **19**, 4723 (1979).
[45] S. Oseroff, S.-W. Cheong, A. Fondado, B. Aktas, and Z. Fisk, J. Appl. Phys. **75**, 6819 (1994).
[46] K. Mortensen, Y. Tomkiewicz, T. D. Schultz, and E. M. Engler, Phys. Rev. Lett. **46**, 1234 (1981); K. Mortensen, Y. Tomkiewicz, and K. Bechgaard, Phys. Rev. B **25**, 3319 (1982).
[47] Details on the antiferromagnetic resonances in the SDW ground state will be presented elsewhere.
[48] C. Bourbonnais, in *Interacting Electrons in Reduced Dimensions*, Vol. 213 of *NATO Advanced Study Institute, Series B: Physics*, edited by D. Baeriswyl and D.K. Campbell (Plenum Press, New York 1989), p. 227.
[49] T. Ogushi, Phys. Rev. **133**, A1098 (1964).
[50] M. Roger, J. M. Delrieu, and E. Wope Mbougue, Phys. Rev. B **34**, 4952 (1986).
[51] C. Bourbonnais and B. Dumoulin, J. Phys. I **6**, 1727 (1996).
[52] J. P. Pouget and S. Ravy, Synth. Met. **85**, 1523 (1997).
[53] P. Baillargeon, C. Bourbonnais, S. Tomić, P. Vaca, and C. Coulon, Synth. Met. **27**, B73 (1988); S. Tomić, J. R. Cooper, W. Kang, D. Jérome, and K. Maki, J. Phys. I **1**, 1603 (1991).
[54] C. Bourbonnais, P. Stein, D. Jérome, and A. Moradpour, Phys. Rev. B **33**, 7608 (1986).
[55] P. Wzietek, C. Bourbonnais, F. Creuzet, D. Jérome, and K. Bechgaard, Europhys. Lett. **12**, 453 (1990).